J. Phys. Chem. A **2003,** *107,* 10171−10176

Theoretical Study of the Fragmentation of the *β*-Lactam Ring: Ozonolysis of 3-Methoxy-4-methyl-*N*-(ethylideneamino)-2-azetidinone

Diego Ardura and Tomás L. Sordo*

Departamento de Química Física y Analítica, Universidad de Oviedo, C/ Julián Clavería, 8, 33006 Oviedo (Spain)

Received: June 24, 2003; In Final Form: September 18, 2003

A theoretical B3LYP/6-31+G* study of the ozonolysis of 3-methoxy-4-methyl-*N*-(ethylideneamino)-2-azetidinone in dichloromethane at 195.15 K, and of the reduction of the corresponding ozonide with BH_4^- in EtOH/H_2O 1:1 at 273.15 K to yield methyl 1-propenyl ether, renders three reaction paths proceeding under the energy level corresponding to reactants in accordance with the exceptionally mild reaction conditions experimentally found. Two of these paths lead to *Z*-methyl 1-propenyl ether with retention of stereochemistry whereas the other one gives *E*-methyl 1-propenyl ether. These theoretical results predict a high level of stereoselectivity in agreement with the experimental values obtained for the synthesis of vinyl ethers from the reaction of *N*-[(arylidene or alkylidene)amino]-2-azetidinones with ozone.

Introduction

In addition to its use in the synthesis of a variety of β-lactam antibiotics, the β-lactam ring is a powerful synthetic building block.[1−4] Opening of the 2-azetidinone ring can be achieved by cleavage of any of the single bonds constituting it. The fragmentation process of *N*-(arylideneamino)- or *N*-(alkylideneamino)-β-lactams, **1**, through the electrophilic attack of ozone yielding vinyl ethers **2** stereoselectively has been reported (see Scheme 1).[5,6] It has been proposed that this process would take place through the electrophilic addition of ozone to form an ozonide intermediate **3**. Decomposition of ^{1}ozonide **3** by the action of $NaBH_4$ could result in the loss of the group attached to the exocyclic nitrogen alcohol and rearrangement to the intermediate **4**, which in turn evolves to intermediate **5** by loss of molecular nitrogen. Alternatively, ozonide **3** may evolve to *N*-nitroso-β-lactam **6** by the effect of $NaBH_4$. Intermediate **6** could yield the final products either by concerted cycloreversion or via hexacyclic intermediate **4** by attack of the oxygen to the lactam carbonyl followed by cleavage of the amide bond of the former β-lactam ring. Vinyl ethers are obtained with moderate to excellent *Z*/*E* selectivities, reflecting the starting 2-azetidinone with important percentages of retention. The good selectivity obtained, which allowed preparing predominantly one of the two isomers across the double bond of the enol ether by selecting the adequate isomer of the starting 2-azetidinone, makes this process an interesting alternative to other synthetic methods for enol ethers. This partial to moderate loss of stereochemical integrity of the starting β-lactam has led to proposing that enol ethers were not formed through a concerted pathway.

In the present work we undertake a theoretical study of the ozonolysis of *N*-[(methylethylene)amino]-2-azetidinone (**1**), and the reduction of the ozonide **3** to give the vinyl ether **2**, trying to disclose the mechanism through which the *Z*/*E* selectivity experimentally found is obtained. We will take into account the effect of solvent in our investigation.

Methods

Quantum chemical computations were performed using the Gaussian 98 series of programs[7] with the hybrid density functional B3LYP method,[8] which combines Becke's three-parameter nonlocal hybrid exchange potential with the nonlocal correlation functional of Lee, Yang, and Parr. The geometries of stable species and transition states (TSs) were fully optimized using the 6-31+G* basis set[9] and Schlegel's algorithm.[10] This theory level seems adequate to study ozonolysis reactions.[11,12] Harmonic vibrational frequencies were also calculated at this same theory level to characterize the critical points located and to evaluate the zero-point vibrational energy (ZPVE). B3LYP/6-31+G* intrinsic reaction coordinate (IRC) calculations starting at each saddle point verified the two minima connected by that TS using the Gonzalez and Schlegel method[13] implemented in Gaussian 98.[14]

Thermodynamic data ΔH, ΔS, and ΔG were computed using the B3LYP/6-31+G* frequencies within the ideal gas, rigid rotor, and harmonic oscillator approximations[15] at 1 atm and 195.15 K for the ozonolysis process, and at 1 atm and 273.15 K for the reduction of the ozonide following experimental conditions.

To take into account the effect of solvent, we used a self-consistent-reaction-field (SCRF) model proposed for quantum chemical computations on solvated molecules.[16−18] The solvent is represented by a dielectric continuum characterized by its relative static dielectric permittivity ϵ_0. The solute, which is placed in a cavity created in the continuum after spending some cavitation energy, polarizes the continuum, which in turn creates an electric field inside the cavity. This interaction can be taken into account by using quantum chemical methods by minimizing the electronic energy of the solute plus the Gibbs energy change

---

* Corresponding author. E-mail: tsordo@correo.uniovi.es.

10.1021/jp035796d CCC: $25.00

SCHEME 1

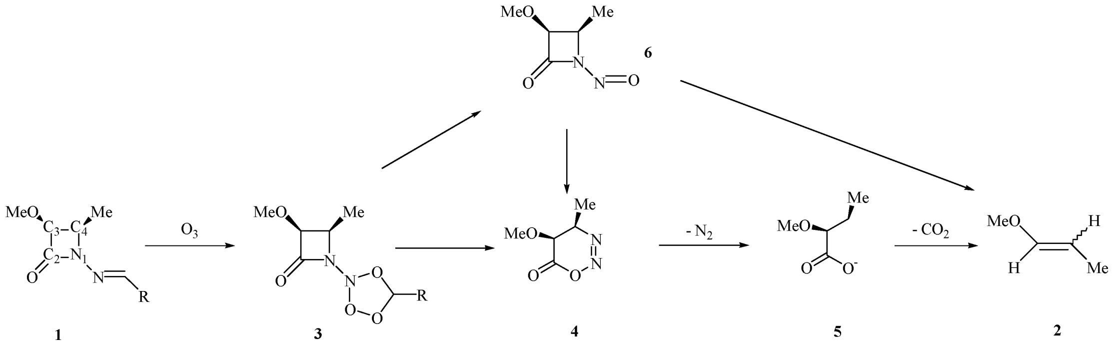

corresponding to the solvation process that is given by

$$\Delta G_{\text{solvation}} = -\frac{1}{2}E_{\text{int}}$$

where E_{int} is the solute−solvent electrostatic interaction energy:

$$E_{\text{int}} = \sum_{a} V_{\text{el}}(R_\alpha)Z_\alpha = -\int V_{\text{el}}(r)\ \rho(r)\ \mathrm{d}r$$

In this equation, V_{el} is the electrostatic potential created by the polarized continuum in the cavity, R_α, and Z_α are the position vector and charge of the nucleus α, respectively, and $\rho(r)$ is the electronic charge density at point r. The factor $-^1/_2$ arises in the Gibbs energy from the fact that the positive work required to polarize the medium is exactly one-half the value of the interaction energy in the linear response approximation. Addition to $\Delta G_{\text{gas-phase}}$ of the solvation Gibbs energy, evaluated by neglecting the change in the relative value of the thermal corrections when going from a vacuum to the solution, gives $\Delta G_{\text{solution}}$. Within the different approaches that can be followed to calculate the electrostatic potential V_{el}, we have employed the united atom Hartree−Fock (UAHF) parametrization of the PCM,[12,15] taking into account electrostatic solute−solvent interactions. The solvation Gibbs energies, $\Delta G_{\text{solvation}}$, along the reaction coordinate were evaluated from single-point PCM-UAHF calculations on the gas-phase optimized geometries. Relative permittivities of 8.93 and 51.47 have been used to simulate dichloromethane and EtOH/H_2O 1:1 employed in the experimental work for the ozonolysis and the reduction processes, respectively.

Results and Discussion

Parts a and b of Figure 1 display the Gibbs energy profiles in solution for the ozonolysis of *N*-[(methylethylene)amino]-2-azetidinone and for the reduction of the corresponding ozonide to yield vinyl ether, respectively. Parts a and b of Figure 2 show the optimized geometries of the critical structures located along the reaction coordinate for ozonolysis and reduction, respectively. Tables 1 and 2 present the relative electronic energies, ZPVEs and Gibbs energies both in the gas phase and in solution corresponding to the two above-mentioned processes. Except otherwise stated, we will give in the text the relative Gibbs energies in solution.

Ozonolysis of 3-Methoxy-4-methyl-*N*-[(methylethylene)-amino]-2-azetidinone. The interaction of O_3 with 3-methoxy-4-methyl-*N*-methylethyleneamino-2-azetidinone leads to the formation of the primary ozonide M1 11.8 kcal/mol more stable than the separate reactants in a barrierless process. M1 evolves through TS12 for the breaking the O−O bond closer to the *β*-lactam ring with an energy barrier of 0.9 kcal/mol to give the intermediate M2 14.8 kcal/mol more stable than reactants. Finally, M2 yields the Criegee intermediates *N*-nitroso-*β*-lactam, M3, and carbonyl oxide, 37.6 kcal/mol more stable than it, without any energy barrier (a transition state TS23 is located for this process in electronic energy in the gas phase but disappears when taking into account the ZPVE correction; see Tables 1 and 2). The Criegee intermediates can react with each other in two different ways. In the first one the carbonyl oxide cycloadds to the N═O bond in the *N*-nitroso-*β*-lactam to give the ozonide M4 through the transition state TS34 with an energy barrier of 25.4 kcal/mol. In the second one the carbonyl oxide cycloadds without energy barrier to the carbonyl group in the *N*-nitroso-*β*-lactam to form the ozonide M7, which is 5.9 kcal/mol below the Criegee intermediates. It is interesting to note that the ozonide appearing in the mechanism previously proposed,[6] M4, cannot kinetically compete with the ozonide M7 located through geometry optimization.

Reduction of the Ozonides with $NaBH_4$. The ozonide M4 would evolve by reaction with $NaBH_4$ yielding the intermediate M5 + $H_3C-CH-OH^-$ + BH_3 through cleavage of the O−O bond by attack of H^- to the endo oxygen atom of the carbonyl dioxide moiety. This cleavage takes place without energy barrier according to our calculations. Barrierless addition of BH_3 to the oxygen atom of the NO_2 moiety endo with respect to the carbonyl group would lead to the adduct M6, which in turn would evolve through the transition state TS63 30.4 kcal/mol above it to render the *N*-nitroso-*β*-lactam M3 + $HOBH_2$ 66.8 kcal/mol more stable than M6. From M3 we located several routes, some of them previously proposed,[6] leading to vinyl ether but these paths proceed through energy barriers of more than 40 kcal/mol and consequently are not competitive with those found from M9 (see below).

The interaction of $NaBH_4$ with ozonide M7 yields the intermediate M8 + BH_3 72.4 kcal/mol under M7 + BH_4^- through H^- attack to the exo oxygen atom of the carbonyl dioxide moiety. Rotation of the N−N−O moiety about the N1−C4 bond renders M9 through the TS TS89, which presents no energy barrier in solution. Extrusion of CH_3CHOH^- from M9 leads to the intermediate M10 with a monotonic increase of Gibbs energy of 4.0 kcal/mol. M10 can evolve through TS1011 to give the intermediate M11 6.4 kcal/mol more stable than it or through TS10P2 for extrusion of N_2 and CO_2 to yield *Z*-vinyl ether. TS1011 and TS10P2 present an electronic energy barrier of 8.6 and 4.8 kcal/mol, respectively, but disappear in solution. M11 can evolve along two different routes. The first one corresponds to a double extrusion process through the TS TS11P1 with an energy barrier of 6.4 kcal/mol to give P1 (*E*-vinyl ether + CO_2 + N_2) 77.1 kcal/mol under M11. At TS11P1 a rotation about the C3−C4 bond takes place, preparing the formation of *E*-vinyl ether, and the C2−C3 bond has elongated

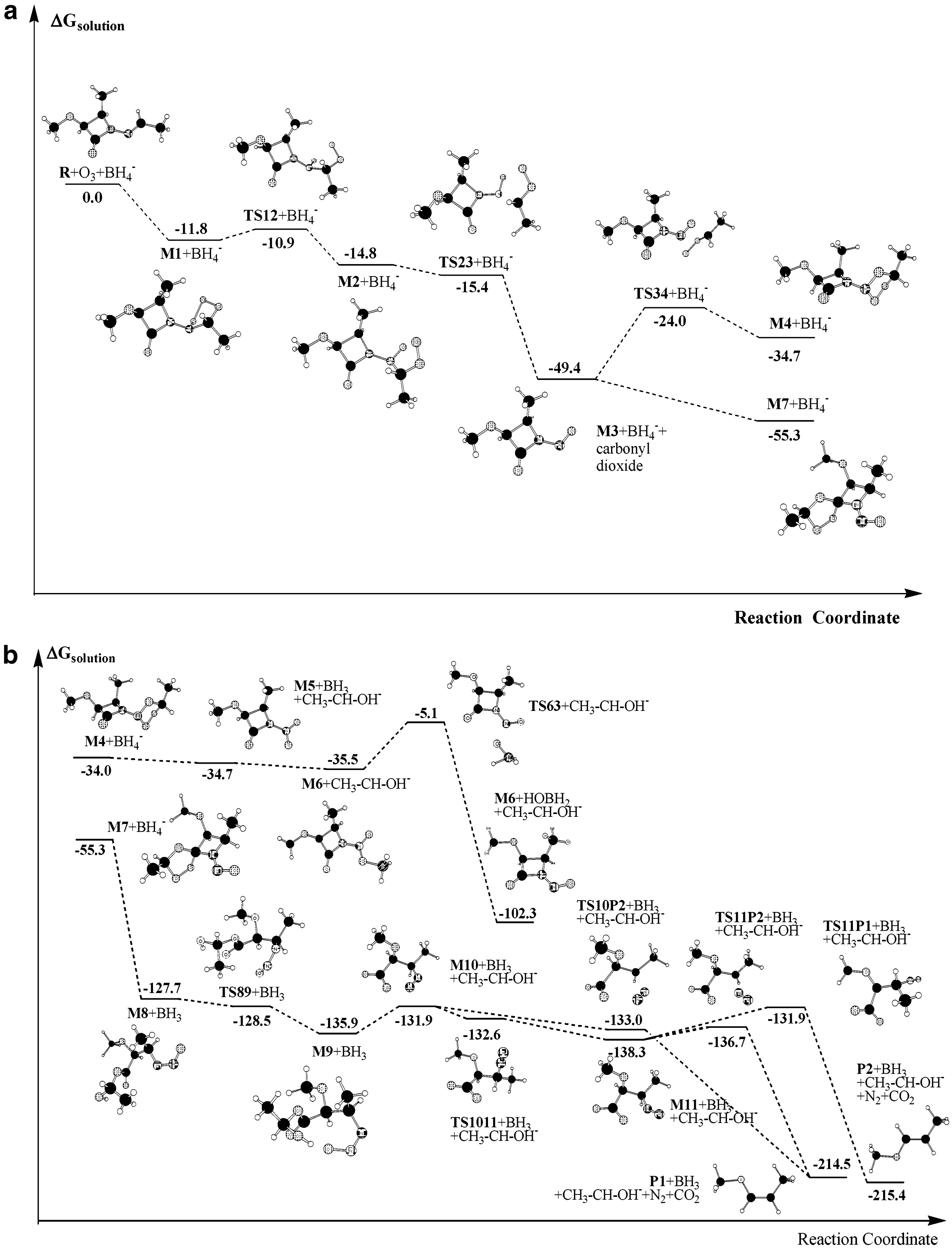

Figure 1. (a) B3LYP/6-31+G* Gibbs energy profile in solution (PCM-UAHF) in kcal/mol for the formation of ozonides in the ozonolysis of 3-metoxy-4-methyl-*N*-(ethylideneamino)-2-azetidinone. (b) B3LYP/6-31+G* Gibbs energy profile in solution (PCM-UAHF) in kcal/mol for the reduction steps of ozonolysis of 3-methoxy-4-methyl-*N*-(ethylideneamino)-2-azetidinone.

up to 1.632 Å for CO$_2$ extrusion. The second route proceeds through the TS TS11P2 with an energy barrier of 1.6 kcal/mol for the extrusion of N$_2$ and CO$_2$, giving rise to *Z*-vinyl ether (P2).

At TS11P2 the C4−N1 and C2−C3 bonds have a value of 1.901 and 1.666 Å, respectively, preparing the extrusion of N$_2$ and CO$_2$.

Comparison with Experiment. The most favorable route located on the B3LYP/6-31+G* potential energy surface proceeding through the ozonide M7 allows us to rationalize the experimental facts previously reported, particularly the *Z*/*E*-vinyl ether ratio obtained experimentally. In effect, the Gibbs energy profile in solution for the process is under the energy level corresponding to separate reactants, and the largest Gibbs energy

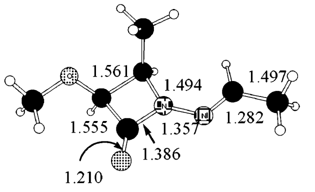

R

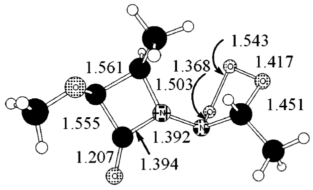

M1

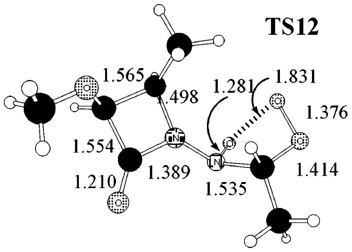

TS12

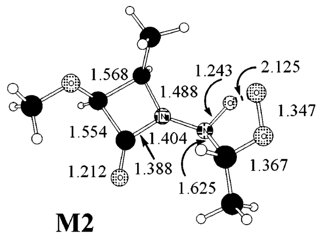

M2

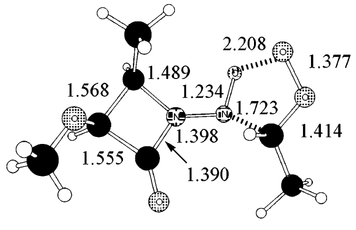

TS23

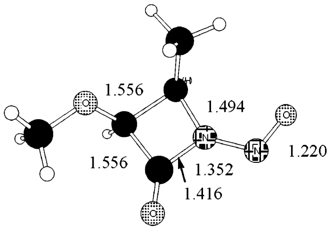

M3

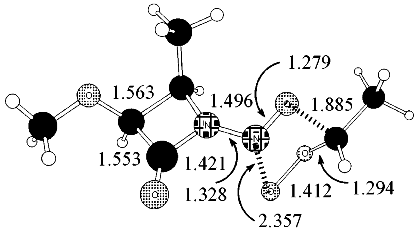

TS34

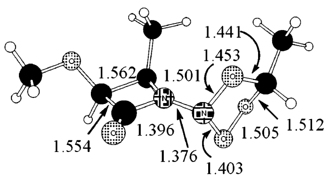

M4

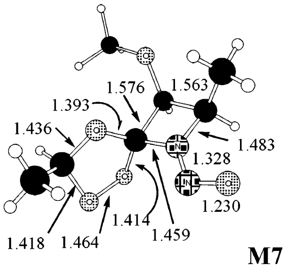

M7

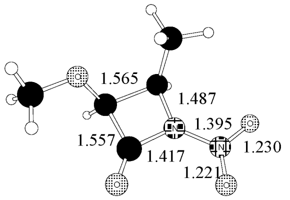

M5

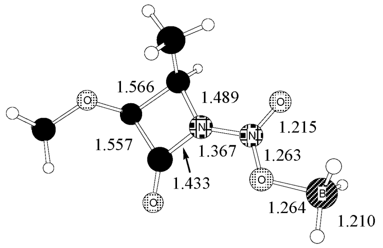

M6

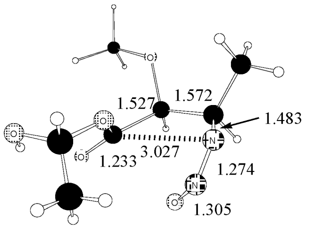

TS89

TS63

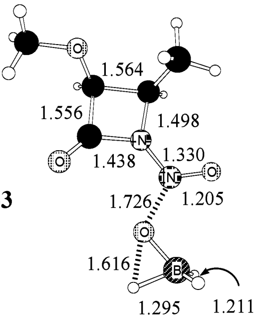

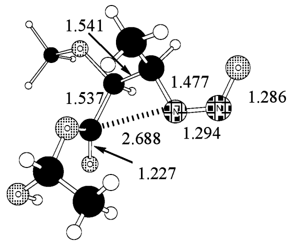

M8

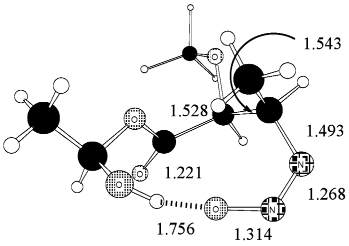

M9

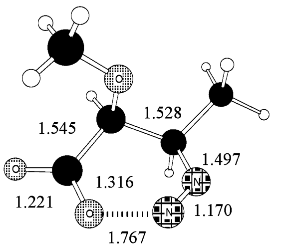

M10

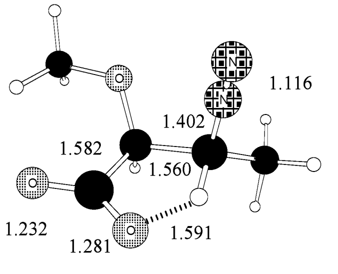

TS1011

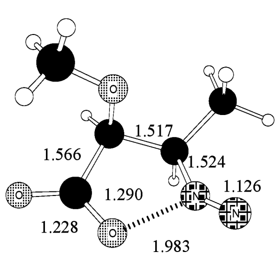

M11

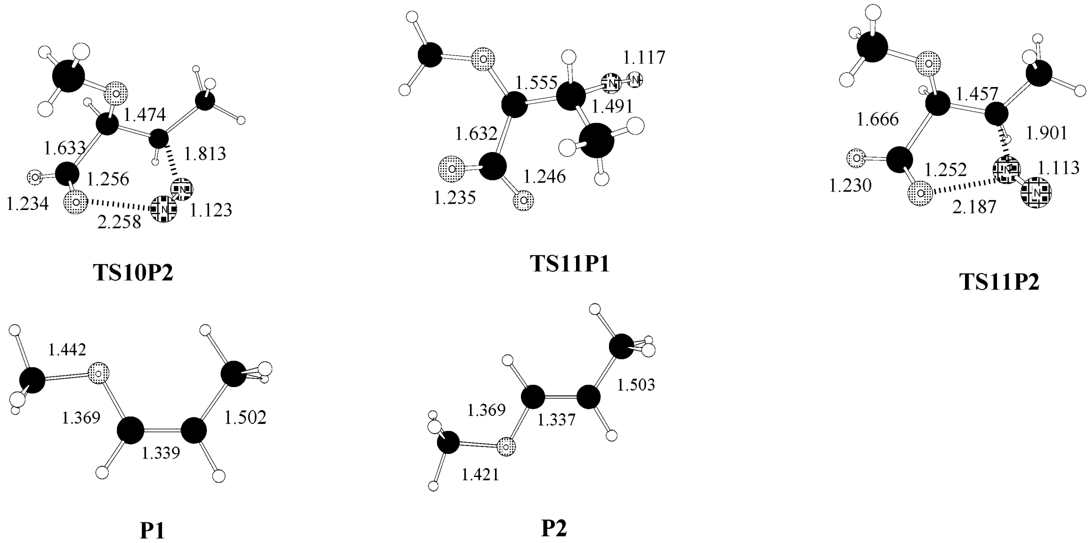

Figure 2. (a) B3LYP/6-31+G* optimized geometries for the structures involved in the first steps of ozonolysis of 3-methoxy-4-methyl-*N*-(ethylideneamino)-2-azetidinone. (b) B3LYP/6-31+G* optimized geometries for the structures involved in the reduction steps of ozonolysis of 3-methoxy-4-methyl-*N*-(ethylideneamino)-2-azetidinone.

TABLE 1: Relative B3LYP/6-31+G* Energies Including ZPVE Correction ($\Delta(E_{elec}$+ZPVE)), Relative ZPVE Corrections (ΔZPVE), Relative Gibbs Free Energies in the Gas Phase ($\Delta G_{gas-phase}$), Relative Gibbs Free Energies of Solvation ($\Delta\Delta G_{solvation}$), and Gibbs Free Energies in Solution ($\Delta G_{solution}$) at 195.15 K, in kcal/mol, for the Structures Involved in the First Steps of Ozonolysis of 3-Methoxy-4-methyl-*N*-(ethylideneamino)-2-azetidinone

structures	ΔE_{elec}	ΔZPVE	$\Delta G_{gas-phase}$	$\Delta\Delta G_{solvation}$	$\Delta G_{solution}$
			Reactants		
$R + O_3 + BH_4^-$	0.0	0.0	0.0	0.0	0.0
			Intermediates		
$M1 + BH_4^-$	−22.6	3.1	−14.6	2.7	−11.8
$M2 + BH_4^-$	−23.6	2.5	−16.0	1.2	−14.8
$M3 + BH_4^-$	−34.6	−0.2	−41.6	−7.8	−49.4
$M4 + BH_4^-$	−44.0	3.3	−36.1	2.1	−34.0
$M7 + BH_4^-$	−65.7	3.8	−57.7	2.3	−55.3
$M3 + HOBH_2 +$ carbonyl dioxide	−107.7	1.7	−112.7	5.75	−107.0
			Transition States		
$TS12 + BH_4^-$	−21.9	2.8	−13.6	2.6	−10.9
$TS23 + BH_4^-$	−24.0	2.0	−16.2	0.7	−15.4
$TS34 + BH_4^-$	−31.1	1.5	−23.6	−0.5	−24.0
$TS63 + CH_3{-}CH{-}OH^-$	−3.7	1.6	−6.9	1.79	−5.1

TABLE 2: Relative B3LYP/6-31+G* Energies Including ZPVE Correction ($\Delta(E_{elec}$+ZPVE)), Relative ZPVE Corrections (ΔZPVE), Relative Gibbs Free Energies in the Gas Phase ($\Delta G_{gas-phase}$), Relative Gibbs Free Energies of Solvation ($\Delta\Delta G_{solvation}$) and Gibbs Free Energies in Solution ($\Delta G_{solution}$) at 273.15 K, in kcal/mol, for the Structures Involved in the Reduction Steps of Ozonolysis of 3-Methoxy-4-methyl-*N*-(ethylideneamino)-2-azetidinone

structures	ΔE_{elec}	ΔZPVE	$\Delta G_{gas-phase}$	$\Delta\Delta G_{solvation}$	$\Delta G_{solution}$
			Intermediates		
$M5 + BH_3 + CH_3{-}CH{-}OH^-$	−26.6	1.3	−38.8	4.12	−34.7
$M6 + CH_3{-}CH{-}OH^-$	−32.1	4.4	−35.0	−0.51	−35.5
$M8 + BH_3$	−148.2	5.5	−149.2	21.43	−127.7
$M9 + BH_3$	−153.9	5.8	−154.0	18.1	−135.9
$M10 + BH_3 + CH_3{-}CH{-}OH^-$	−122.3	1.7	−134.2	2.4	−131.9
$M11 + BH_3 + CH_3{-}CH{-}OH^-$	−124.6	1.7	−136.8	−1.5	−138.3
			Transition States		
$TS89 + BH_3$	−144.3	5.7	−143.5	15.0	−128.5
$TS1011 + BH_3 + CH_3{-}CH{-}OH^-$	−113.7	−0.6	−125.9	−6.7	−132.6
$TS11P2 + BH_3 + CH_3{-}CH{-}OH^-$	−121.6	−0.7	−134.3	−2.3	−136.7
$TS10P2 + BH_3 + CH_3{-}CH{-}OH^-$	−117.5	−0.6	−129.8	−3.2	−133.0
$TS11P1 + BH_3 + CH_3{-}CH{-}OH^-$	−108.2	0.1	−120.2	−11.7	−131.9
			Products		
$P1 + BH_3 + CH_3{-}CH{-}OH^-$	−196.0	−4.2	−224.4	9.0	−215.4
$P2 + BH_3 + CH_3{-}CH{-}OH^-$	−195.5	−4.4	−223.0	8.5	−214.5

barrier appearing along the reaction coordinate is of 6.4 kcal/mol (TS11P1). This is in accordance with the experimental observation that this reaction takes place in exceptionally mild reaction conditions.

On the other hand, we found three different routes yielding vinyl ether from the reduction of M7. Two of them render the *Z* isomer with retention of the original configuration whereas the remaining one yields the *E* isomer. Then our theoretical calculations predict high levels of stereoselectivity of the order of *Z*/*E* 67/33, in agreement with the experimental values obtained for the synthesis of vinyl ethers from the reaction of *N*-[(arylidene or alkylidene)amino]-2-azetidinones with ozone.[5,6]

It is interesting to note that no intermediate zwitterion **5** (see Scheme 1) has been located on the potential energy surface. The search for **5** failed even when geometry optimization was allowed in solution.

In summary, a theoretical B3LYP/6-31+G* study of the ozonolysis of 3-methoxy-4-methyl-*N*-(ethylideneamino)-2-azetidinone yields as the most favorable route that passing through the ozonide M7, in contrast with previous proposals. The reduction of ozonide M7 yields the enol ether **2** (see Scheme 1) through three reaction paths proceeding under the energy level corresponding to reactants. Two of these routes lead to *Z*-vinyl ether with retention of stereochemistry whereas the other one gives *E*-vinyl ether, in agreement with experimental findings.

Acknowledgment. We thank DGESIC (Spain) (SAF2001-3596) and Principado de Asturias ((PB02-045) for financial support.

References and Notes

(1) *The Organic Chemistry of β-Lactams*; Georg, G. I., Ed.; VCH: New York, 1993.

(2) Ojima, I.; Hatanaka, N. *J. Synth. Org. Chem., Jpn.* **1982**, *40*, 209.

(3) Ojima, I. In *Asymmetric Reactions and Processes in Chemistry*; Eliel, E. L., Otsuka, S., Eds.; ACS Symposium Series 185; American Chemical Society: Washington, DC, 1982: pp 109−138.

(4) Wasserman, H. H.; Leadbetter, M. R.; Kopka, I. E. *Tetrahedron Lett.* **1984**, *25*, 2391. Wasserman, H. H.; Robinson, R. T. *Tetrahedron Lett.* **1983**, *24*, 3669. Wasserman, H. H.; Berger, G. D.; Cho, K. R. *Tetrahedron Lett.* **1982**, *23*, 465. Wasserman, H. H.; Matsuyama, H. *J. Am. Chem. Soc.* **1981**, *103*, 461. Sagarovi, H. U.; Fitzpatrick, D.; Raktabutr, A.; Nakanishi, H.; Kahn, M.; Greene, M. I. *Science* **1991**, *253*, 792.

(5) Alcaide B.; Miranda, M.; Pérez-Castells, J.; Sierra, M. A. *J. Org. Chem.* **1993**, *58*, 297.

(6) Alcaide, B.; Pérez-Castells, Polanco, C.; Sierra, M. A. *J. Org. Chem.* **1995**, *60*, 6012.

(7) Frisch, M. J.; Trucks, G. W.; Schlegel, H. B.; Scuseria, G. E.; Robb, M. A.; Cheeseman, J. R.; Zakrzewski, V. G.; Montgomery, J. A., Jr.; Stratmann, R. E.; Burant, J. C.; Dapprich, S.; Millam, J. M.; Daniels, A. D.; Kudin, K. N.; Strain, M. C.; Farkas, O.; Tomasi, J.; Barone, V.; Cossi, M.; Cammi, R.; Mennucci, B.; Pomelli, C.; Adamo, C.; Clifford, S.; Ochterski, J.; Petersson, G. A.; Ayala, P. Y.; Cui, Q.; Morokuma, K.; Malick, D. K.; Rabuck, A. D.; Raghavachari, K.; Foresman, J. B.; Cioslowski, J.; Ortiz, J. V.; Stefanov, B. B.; Liu, G.; Liashenko, A.; Piskorz, P.; Komaromi, I.; Gomperts, R.; Martin, R. L.; Fox, D. J.; Keith, T.; Al-Laham, M. A.; Peng, C. Y.; Nanayakkara, A.; Gonzalez, C.; Challacombe, M.; Gill, P. M. W.; Johnson, B.; Chen, W.; Wong, M. W.; Andres, J. L.; Gonzalez, C.; Head-Gordon, M.; Replogle, E. S.; Pople, J. A. *Gaussian98*; Gaussian, Inc.: Pittsburgh, PA, 1998.

(8) (a) Becke, A. D. *Phys. Rev. A* **1988**, *38*, 3098−3100. (b) Lee, C.; Yang, W.; Parr, R. G. *Phys. Rev. B* **1988**, *37*, 785−789. (c) Becke, A. D. *J. Chem. Phys.* **1993**, *98*, 5648−5652.

(9) Hehre, W. J.; Radom, L.; Pople, J. A.; Schleyer, P. v. R. *Ab Initio Molecular Orbital Theory*; John Wiley & Sons Inc.: New York, 1986.

(10) Schlegel, H. B. *J. Comput. Chem.* **1982**, *3*, 214−218.

(11) Olzmann, M.; Kraka, E.; Cremer, D.; Gutbrod, R.; Andersson, S. *J. Phys. Chem. A* **1997**, *101*, 9421−9429.

(12) Gutbrod, R.; Kraka, E.; Schindler, R. N.; Cremer, D. *J. Am. Chem. Soc.* **1997**, *119*, 7330−7342.

(13) (a) Gonzalez, C.; Schlegel, H. B. *J. Chem. Phys.* **1989**, *90*, 2154−2161. (b) Gonzalez, C.; Schlegel, H. B. *J. Phys. Chem.* **1990**, *94*, 5523−5527.

(14) IRC calculations from TS1011 failed. However, the connection between this TS and M10 and M11 intermediates was checked by relocating TS1011 from these intermediates using the QST2 method.

(15) McQuarrie, D. A. *Statistical Mechanics*; Harper & Row: New York, 1976.

(16) Rivail, J. L.; Rinaldi, D.; Ruiz-López, M. F. In *Theoretical and Computational Model for Organic Chemistry*; Formosinho, S. J., Csizmadia, I. G., Arnaut, L., Eds.: NATO ASI Series C.; Kluwer Academic Publishers: Dordrecht, The Netherlands, 1991; Vol. 339, pp 79−92.

(17) (a) Tomasi, J.; Persico, M. *Chem. Rev.* **1994**, *94*, 2027−2094. (b) Cammi, R.; Tomasi, J. *J. Comput. Chem.* **1995**, *16*, 1449−1458.

(18) Cramer, C. J.; Truhlar, D. G. *Chem. Rev.* **1999**, *99*, 2161−2200.